Superfluid density and specific heat within a self-consistent scheme for a two-band superconductor

V. G. Kogan,* C. Martin,† and R. Prozorov‡
Department of Physics & Astronomy and Ames Laboratory, Iowa State University, Ames, Iowa 50011, USA
(Received 1 May 2009; published 9 July 2009)

The two gaps in a two-band clean *s*-wave superconductor are evaluated self-consistently within the quasiclassical Eilenberger weak-coupling formalism with two in-band and one interband pairing potentials. Superfluid density, free energy, and specific heat are given in the form amenable for fitting the experimental data. Well-known two-band MgB_2 and V_3Si superconductors are used to test the developed approach. The pairing potentials obtained from the fit of the superfluid density data in MgB_2 crystal were used to calculate temperature-dependent specific heat $C(T)$. The calculated $C(T)$ compares well with the experimental data. Advantages and validity of this, which we call the "γ model," are discussed and compared with the commonly used empirical (and not *self-consistent*) "α model." Correlation between the sign of the interband coupling and the signs of the two order parameters is discussed. Suppression of the critical temperature by the interband scattering is evaluated and shown to be severe for the interband repulsion as compared to the attraction. The data on a strong T_c suppression in MgB_2 crystals by impurities suggest that the order parameters on two effective bands of this material may have opposite signs, i.e., may have the $s_{\pm}$ structure similar to proposals for iron-based pnictide superconductors.

DOI: 10.1103/PhysRevB.80.014507 PACS number(s): 74.25.Nf, 74.20.Rp, 74.20.Mn

I. INTRODUCTION

Nearly all superconductors discovered recently and some well-studied compounds (e.g., MgB_2, Nb_2Se, V_3Si, and ZrB_{12}) (Refs. 1–5) are multiband materials with complex Fermi surfaces and anisotropic order parameters. Measuring temperature dependences of the London penetration depth $\lambda(T)$, often converted to the superfluid density $\rho(T)=\lambda(0)^2/\lambda(T)^2$, and of the electronic specific heat $C(T)$, are among primary tests directly linked to pairing mechanisms of new superconductors. Still, the methods employed to interpret the data are often empiric with simplicity as a main justification.

The most popular among practitioners α model takes a shortcut by assigning the BCS temperature dependence to the two gaps $\Delta_{1,2}$ with which to fit data on the specific heat[1] and the superfluid density $\rho=x\rho_1+(1-x)\rho_2$.[2,6] Here, $\rho_{1,2}$ are evaluated with $\Delta_{1,2}=(\alpha_{1,2}/1.76)\Delta_{BCS}(T)$ and x takes into account the relative band contributions. Although the α model had played an important and timely role in providing convincing evidence for the two-gap superconductivity in MgB_2,[1,2] it is intrinsically inconsistent in the most important task of this procedure, namely, in describing properly the temperature dependencies of $\rho(T)$ and $C(T)$. In fact, one cannot *a priori* assume temperature dependencies for the gaps in the presence of, however, weak interband coupling imposing the same T_c for two bands. In an unlikely situation of zero interband coupling, two gaps would have single-gap BCS-type T dependencies but will have two different transition temperatures (see Fig. 1).

The full-blown microscopic approach based on the Eliashberg theory, on the other hand, is quite involved and not easy for the data analysis.[7–12] Hence, the need for a relatively simple but justifiable, self-consistent, and effective scheme experimentalists could employ. The weak-coupling model is such a scheme. Over the years, the weak-coupling theory had proven to describe well the multitude of superconducting phenomena. Similar to the weak coupling is the "renormalized BCS" model of Ref. 13 that incorporates the Eliashberg corrections in the effective coupling constants in a manner described below. We will call our approach as a "weak-coupling two-band scheme" and clarify in the text below that the applicability of the model for the analysis of the superfluid density and specific-heat data is broader than the traditional weak coupling.

The *s*-wave weak-coupling multigap model has been proposed at the dawn of superconductivity theory by Moskalenko[14] and Suhl *et al.*[15] when numerical tools were still in infancy. In this work, we basically follow these seminal publications to develop a self-consistent procedure for the penetration-depth data analysis. Our scheme allows one to connect between two independent data sets—the super-

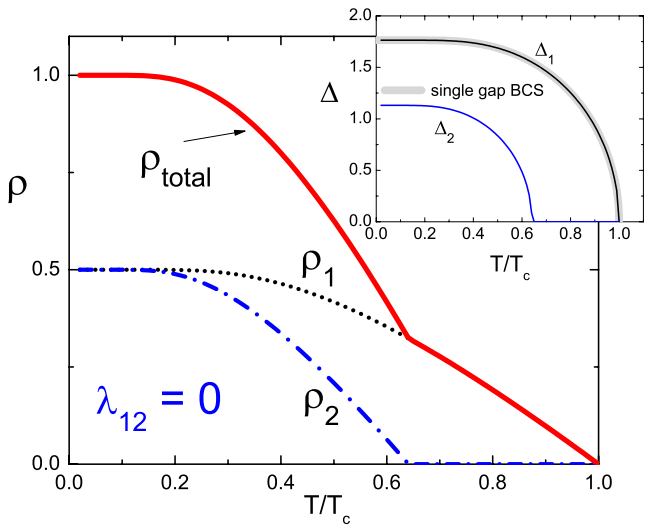

FIG. 1. (Color online) Calculated superfluid density and the gaps vs the reduced temperature (inset) for zero interband coupling $\lambda_{12}=0$. In this calculation, $\lambda_{11}=0.5$, $\lambda_{22}=0.45$, $n_1=n_2=0.5$, and $\gamma=0.5$ (see the text).

fluid density and the specific heat—thus providing a reliability check upon values of the coupling constants extracted from fitting the data. We also discuss the suppression of the critical temperature T_c by nonmagnetic impurities and suggest that the data on this suppression for MgB_2 are consistent with a weak repulsive interband interaction that corresponds to opposite signs of the order parameter on two bands, i.e., to $\pm s$ structure of the order parameter.

To test our formal scheme, the data for two known s-wave two-gap superconductors MgB_2 and V_3Si were used. The specific-heat data were taken from Ref. 16. The penetration depth $\lambda(T)$ was measured by using a self-oscillating tunnel-diode resonator (TDR) with resonant frequency $f_0 \approx 14$ MHz. The measured quantity is the shift of this frequency $f(T)-f_0=-4\pi\chi(T)\mathcal{G}$, where χ is the total magnetic susceptibility in the Meissner state and $\mathcal{G}\simeq f_0 V_s/2V_c(1-N)$ is a geometric factor defined by volumes of the coil V_c and of the sample V_s and by the demagnetization factor N. The factor $\mathcal{G}$ is measured directly by pulling the sample out of the coil at the lowest temperature.[6] For the susceptibility, we use $4\pi\chi=(\lambda/w)[\tanh(w/\lambda)-1]$, where w is a characteristic sample size.[17]

II. EILENBERGER TWO-BAND SCHEME

Perhaps, the simplest formally weak-coupling approach is based on the Eilenberger quasiclassical formulation of the superconductivity valid for general anisotropic order parameters and Fermi surfaces.[18] Eilenberger functions f,g for clean materials in equilibrium obey the system,

$$0 = 2\Delta g/\hbar - 2\omega f, \tag{1}$$

$$g^2 = 1 - f^2, \tag{2}$$

$$\Delta(\mathbf{k}) = 2\pi T N(0) \sum_{\omega>0}^{\omega_D} \langle V(\mathbf{k},\mathbf{k}') f(\mathbf{k}',\omega)\rangle_{\mathbf{k}'}. \tag{3}$$

Here, $\mathbf{k}$ is the Fermi momentum; Δ is the gap function which may depend on the position $\mathbf{k}$ at the Fermi surface in cases other than the isotropic s wave. Further, $N(0)$ is the total density of states at the Fermi level per one spin; the Matsubara frequencies are defined by $\hbar\omega=\pi T(2n+1)$ with an integer n, and ω_D is the Debye frequency; and $\langle\ldots\rangle$ stands for averages over the Fermi surface. As a *weak-coupling* theory, the Eilenberger scheme deals with the *effective electron-electron* coupling V responsible for superconductivity; properties of intermediate bosons (phonons or other possible mediators) enter via properly renormalized V.

Consider a model material with the gap given by

$$\Delta(\mathbf{k}) = \Delta_{1,2}, \quad \mathbf{k} \in F_{1,2}, \tag{4}$$

where F_1, F_2 are two sheets of the Fermi surface. The gaps are constant at each band. Denoting the densities of states on the two parts as $N_{1,2}$, we have for a quantity X constant at each Fermi sheet,

$$\langle X\rangle = (X_1 N_1 + X_2 N_2)/N(0) = n_1 X_1 + n_2 X_2, \tag{5}$$

where $n_{1,2}=N_{1,2}/N(0)$; clearly, $n_1+n_2=1$.

Equations (1) and (2) are easily solved. Within the two-band model, we have

$$f_\nu = \frac{\Delta_\nu}{\beta_\nu}, \quad g_\nu = \frac{\hbar\omega}{\beta_\nu}, \quad \beta_\nu^2 = \Delta_\nu^2 + \hbar^2\omega^2, \tag{6}$$

where the band index $\nu=1,2$. The self-consistency equation (3) takes the form

$$\Delta_\nu = 2\pi T \sum_{\mu=1,2} n_\mu \lambda_{\nu\mu} f_\mu = \sum_\mu n_\mu \lambda_{\nu\mu}\Delta_\mu \sum_\omega^{\omega_D} \frac{2\pi T}{\beta_\mu}, \tag{7}$$

where $\lambda_{\nu\mu}=N(0)V(\nu,\mu)$ are dimensionless effective interaction constants.

A remark is here in order about applicability of Eq. (7) central to our approach. Starting with the general Eliashberg formalism, Nicol and Carbotte derived a renormalized BCS self-consistency equation[13]

$$\Delta_\nu = \frac{2\pi T}{Z_\nu} \sum_{\mu,\omega}^{\omega_D} (\lambda_{\nu\mu}^{ph} - \mu_{\nu\mu}^*) f_\mu, \tag{8}$$

where $\lambda_{\nu\mu}^{ep}$ is the coupling due to electron-phonon interaction, $\mu_{\nu\mu}^*$ describes the Coulomb interaction, and $Z_\nu=1+\Sigma_\mu\lambda_{\nu\mu}^{ep}$ is the strong-coupling renormalization. Replacing $(\lambda_{\nu\mu}^{ep}-\mu_{\nu\mu}^*)/Z_\nu \to n_\nu\lambda_{\nu\mu}$, we obtain our Eq. (7). One should have this in mind while interpreting the constants $\lambda_{\nu\mu}$, which can be obtained from fitting the data to our renormalized weak-coupling model.

Note that the notation commonly used in literature for $\lambda_{\nu\mu}^{(lit)}$ differs from ours: $\lambda_{\nu\mu}^{(lit)}=n_\mu\lambda_{\nu\mu}$. We find our notation convenient since, being proportional to the coupling potential, our coupling matrix is symmetric: $\lambda_{\nu\mu}=\lambda_{\mu\nu}$. It is worth stressing that for a given coupling matrix $\lambda_{\mu\nu}$, relative densities of states n_ν, and the energy scale $\hbar\omega_D$, Eq. (7) determines both T_c and $\Delta_{1,2}(T)$.

A. Critical temperature T_c

As $T\to T_c$, $\Delta_{1,2}\to 0$, and $\beta\to\hbar\omega$. The sum over ω in Eq. (7) is readily evaluated,

$$S = \sum_\omega^{\omega_D} \frac{2\pi T}{\hbar\omega} = \ln\frac{2\hbar\omega_D}{T_c\pi e^{-\gamma}} = \ln\frac{2\hbar\omega_D}{1.76T_c}, \tag{9}$$

$\gamma=0.577$ is the Euler constant. This relation can also be written as

$$1.76T_c = 2\hbar\omega_D e^{-S}. \tag{10}$$

The system (7) is linear and homogeneous,

$$\Delta_1 = S(n_1\lambda_{11}\Delta_1 + n_2\lambda_{12}\Delta_2),$$

$$\Delta_2 = S(n_1\lambda_{12}\Delta_1 + n_2\lambda_{22}\Delta_2). \tag{11}$$

It has nontrivial solutions $\Delta_{1,2}$ if its determinant is zero,

$$S^2 n_1 n_2 \eta - S(n_1\lambda_{11} + n_2\lambda_{22}) + 1 = 0,$$

$$\eta = \lambda_{11}\lambda_{22} - \lambda_{12}^2. \tag{12}$$

The roots of this equation are

$$S = \frac{n_1\lambda_{11} + n_2\lambda_{22} \pm \sqrt{(n_1\lambda_{11} + n_2\lambda_{22})^2 - 4n_1n_2\eta}}{2n_1n_2\eta},$$

$$= \frac{n_1\lambda_{11} + n_2\lambda_{22} \pm \sqrt{(n_1\lambda_{11} - n_2\lambda_{22})^2 + 4n_1n_2\lambda_{12}^2}}{2n_1n_2\eta}. \quad (13)$$

Since $T_c \ll \hbar\omega_D$, Eq. (10) shows that only positive S are admissible. The second form [Eq. (13)] shows that both roots are real; their product is $S_1S_2 = 1/n_1n_2\eta$. Choosing a proper root, one should consider various possibilities.

If $\eta > 0$ (that implies both λ_{11} and λ_{22} are of the same sign), Eq. (13) shows that both roots are positive and one should choose the smallest (to have maximum T_c). If $\eta < 0$ [$\lambda_{12}^2 > \lambda_{11}\lambda_{22}$ that can happen (i) for a sufficiently strong interband coupling for both λ_{11} and λ_{22} positive or (ii) if one of λ_{11}, λ_{22} is repulsive], one should take the square root with *minus*.

It is of interest to note that even for $\lambda_{11} = \lambda_{22} = 0$, the interband coupling of either sign may lead to superconductivity. In fact, $S = 1/\sqrt{n_1n_2}|\lambda_{12}|$ for a dominant interband interaction $|\lambda_{12}| \gg |n_1\lambda_{11} + n_2\lambda_{22}|$. However exotic, this possibility should not be ignored. This situation has been considered time ago by Geilikman[19] who found that interband Coulomb repulsion could lead to superconductivity; recently this possibility has been considered by Mazin and Schmalian in a discussion of superconductivity in the iron pnictides.[20]

If $\eta = 0$, Eq. (12) yields $S = 1/(n_1\lambda_{11} + n_2\lambda_{22})$. Finally, if the interband coupling is exactly zero, a quite unlikely situation, the second form of S in Eq. (13) gives two roots $1/n_1\lambda_{11}$ and $1/n_2\lambda_{22}$. The smallest one gives T_c, whereas the other corresponds to the temperature at which the small gap turns zero. This situation is depicted in Fig. 1.

We conclude this incomplete list of possibilities by noting that within this model, interband coupling enters S only as λ_{12}^2, i.e., interband attraction in clean materials affects T_c exactly as does the repulsion. This is no longer true in the presence of interband scattering, the question discussed below.

Denoting the properly chosen root as $S = 1/\tilde{\lambda}$, we have

$$1.76T_c = 2\hbar\omega_D \exp(-1/\tilde{\lambda}). \quad (14)$$

One easily checks that for all λ's equal this yields the standard BCS result. Among various possibilities we mention here, the case $\eta = \lambda_{11}\lambda_{22} - \lambda_{12}^2 = 0$ for which

$$\tilde{\lambda} = n_1\lambda_{11} + n_2\lambda_{22} = \langle\lambda\rangle. \quad (15)$$

This case corresponds to a popular model with factorizable coupling potential $V(\boldsymbol{k},\boldsymbol{k}') = V_0\Omega(\boldsymbol{k})\Omega(\boldsymbol{k}')$.[21] This potential is amenable for the analytic work, but it curtails severely the richness of the two-band scheme.

Since the determinant of the system (11) is zero, the two equations are equivalent and give near T_c,

$$\frac{\Delta_2}{\Delta_1} = \frac{\tilde{\lambda} - n_1\lambda_{11}}{n_2\lambda_{12}}. \quad (16)$$

When the right-hand side is negative, Δ's are of opposite signs. Within the one-band BCS, the sign of Δ is a matter of convenience; in fact for one band, the self-consistency equation determines only $|\Delta|$. For two bands, Δ_1 and Δ_2 may have opposite signs. If the Δ values are $+D_1$ and $-D_2$, Eq. (7) shows that $-D_1$ and $+D_2$ is a solution too. One should be aware of this multiplicity of solutions when solving the system (7) numerically. The problem is even worse because $\Delta_1 = \Delta_2 = 0$ is always a solution.

B. Order parameter

Turning to evaluation of $\Delta_\nu(T)$, we note that the sum in Eq. (7) is logarithmically divergent. To deal with this difficulty, we employ Eilenberger's idea of replacing $\hbar\omega_D$ with the measurable T_c. These are related by Eq. (14) which can be written as

$$\frac{1}{\tilde{\lambda}} = \ln\frac{T}{T_c} + \sum_{\omega}^{\omega_D} \frac{2\pi T}{\hbar\omega}. \quad (17)$$

Now add and subtract, the last sum from one in Eq. (7),

$$\Delta_\nu = \sum_\mu n_\mu\lambda_{\nu\mu}\Delta_\mu\left[\sum_{\omega}^{\omega_D}\left(\frac{2\pi T}{\beta_\mu} - \frac{2\pi T}{\hbar\omega}\right) + \sum_{\omega}^{\omega_D}\frac{2\pi T}{\hbar\omega}\right],$$

$$= \sum_\mu n_\mu\lambda_{\nu\mu}\Delta_\mu\left[\sum_{\omega}^{\infty}\left(\frac{2\pi T}{\beta_\mu} - \frac{2\pi T}{\hbar\omega}\right) + \frac{1}{\tilde{\lambda}} - \ln\frac{T}{T_c}\right]. \quad (18)$$

The last sum over ω is fast converging and one can replace ω_D with ∞. Numerically, the upper limit of summation over n can be set as a few hundreds that suffices even for low temperatures. Introducing dimensionless quantities

$$\delta_\nu = \frac{\Delta_\nu}{2\pi T} = \frac{\Delta_\nu}{T_c}\frac{1}{2\pi t}, \quad (19)$$

with $t = T/T_c$, we rewrite Eq. (18),

$$\delta_\nu = \sum_{\mu=1,2} n_\mu\lambda_{\nu\mu}\delta_\mu\left(\frac{1}{\tilde{\lambda}} + \ln\frac{T_c}{T} - A_\mu\right),$$

$$A_\mu = \sum_{n=0}^{\infty}\left(\frac{1}{n+1/2} - \frac{1}{\sqrt{\delta_\mu^2 + (n+1/2)^2}}\right). \quad (20)$$

For given coupling constants $\lambda_{\nu\mu}$ and densities of states n_ν, this system can be solved numerically for δ_ν and therefore provide the gaps $\Delta_\nu = 2\pi T\delta_\nu(t)$. Two examples of these solutions with the sets of parameters differing only in λ_{12} are given in insets to Figs. 1 and 2. We observe that even a small interband coupling changes drastically the behavior of the small gap.

C. Superfluid density

Having formulated the way to evaluate $\Delta(T)$, we turn to the London penetration depth given for general anisotropies of the Fermi surface and of Δ by (see, e.g., Ref. 22)

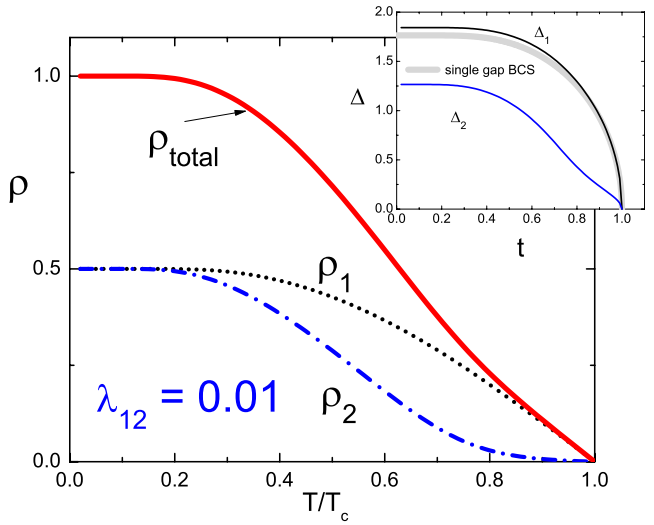

FIG. 2. (Color online) Calculated superfluid density and the gaps vs the reduced temperature (inset) for $\lambda_{12}=0.01$, $\lambda_{11}=0.5$, $\lambda_{22}=0.45$, $n_1=n_2=0.5$, and $\gamma=0.5$ (see the text).

$$(\lambda_L^2)_{ik}^{-1} = \frac{16\pi^2 e^2 N(0) T}{c^2} \sum_{\omega} \left\langle \frac{\Delta_0^2 v_i v_k}{\beta^3} \right\rangle, \tag{21}$$

where v_i is the Fermi velocity. We consider here only the case of currents in the *ab* plane of uniaxial or cubic materials with two separate Fermi-surface sheets, for which a simple algebra gives for the superfluid density $\rho=\lambda_{ab}^2(0)/\lambda_{ab}^2(T)$,

$$\rho = \gamma\rho_1 + (1-\gamma)\rho_2,$$

$$\rho_\nu = \delta_\nu^2 \sum_{n=0}^{\infty} [\delta_\nu^2 + (n+1/2)^2]^{-3/2},$$

$$\gamma = \frac{n_1 v_1^2}{n_1 v_1^2 + n_2 v_2^2}, \tag{22}$$

where v_ν^2 are averages over corresponding band of the in-plane Fermi velocities. The formal similarity of the first line here to the widely used α model prompts to name our scheme as the γ model. We note, however, that these models are quite different: our γ that determines partial contributions from each band is not just a partial density of states n_1 of the α model, instead it involves the band's Fermi velocities; besides, we do not use renormalized BCS gaps, instead we calculate $\Delta_{1,2}(T)$ self-consistently.

We now apply the approach developed to fit the data for the superfluid density of MgB_2 crystals acquired by using the TDR technique described above. Figure 3 shows the result of the fitting with three free parameters λ_{11}, λ_{22}, and λ_{12}. The partial density of states and the parameter γ were taken from the literature: the two-band mapping of the four-band MgB_2 gives $n_1=0.44$ and the Fermi velocities $\langle v_{ab}^2\rangle_1=3.3$ and $\langle v_{ab}^2\rangle_2=2.3\times10^{15}$ cm^2/s^2.[23,24] The fit requires solving two coupled nonlinear equation (20). We used MATLAB with the OPTIMIZATION TOOLBOX and utilized a nonlinear solver using direct Nelder-Mead simplex search method.[25] The result is

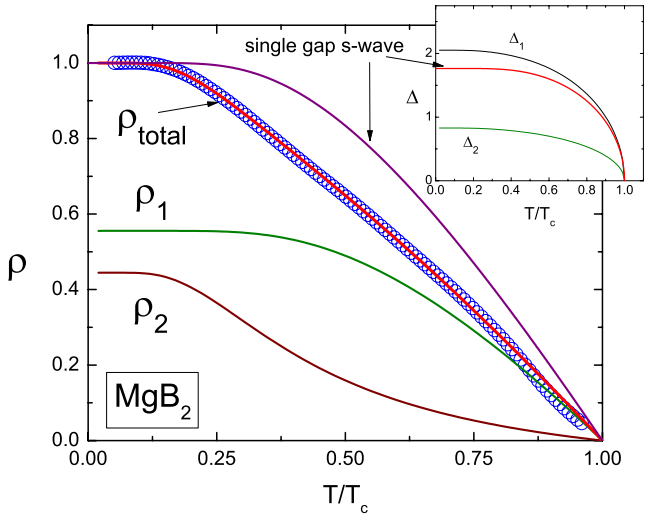

FIG. 3. (Color online) The data and fits of the superfluid density for MgB_2 single crystal and corresponding temperature-dependent gaps (inset). The fitting parameters are $\lambda_{11}=0.23$, $\lambda_{22}=0.08$, and $\lambda_{12}=0.06$; the partial density of states $n_1=0.44$ and $\gamma=0.56$ were fixed.

shown in Fig. 3 with the best-fit parameters listed in the caption. We show below that the same set of parameters used to calculate the free energy and the specific heat reproduces the data on $C(T)$ remarkably well.

Our numerical experimentation shows that if, in addition to coupling constants, the partial densities of states and the Fermi velocities are also used as fit parameters, the numerical procedure becomes unstable and equally good fits can be found for various combinations of fit parameters. In the case of MgB_2, n_ν and v_ν are known and our fitting is quite certain. For V_3Si, we do not have detailed information regarding the band structure, partial densities of states, and Fermi velocities on separate sheets of the Fermi surface. Hence, we took all those as free parameters in the fitting procedure. The conclusions thus are less reliable for this material than for MgB_2: being mapped onto a two-band model, V_3Si comes out to have two nearly decoupled bands with an extremely weak interband coupling (still sufficient to give a single T_c). The results and the best-fit parameters are given in the caption of Fig. 4. Note that the long linear tail in $\rho(t)$ as T approaches T_c is a direct manifestation of a very small gap, in this case Δ_1, in this temperature domain.

III. FREE ENERGY AND SPECIFIC HEAT

By fitting the data for $\rho(t)$, we can extract the coupling constants $\lambda_{\nu\mu}$ along with $\Delta_\nu(T)$. This allows one to determine all thermodynamic properties of the material in question, of which we consider here the specific heat $C(T)$ and its jump at T_c. To this end, one starts with the Eilenberger expression for the energy difference,

$$\frac{F_n - F_s}{N(0)} = 2\pi T \sum_{\nu,\omega} n_\nu \frac{(\beta_\nu - \hbar\omega)^2}{\beta_\nu}. \tag{23}$$

Near T_c, one obtains,

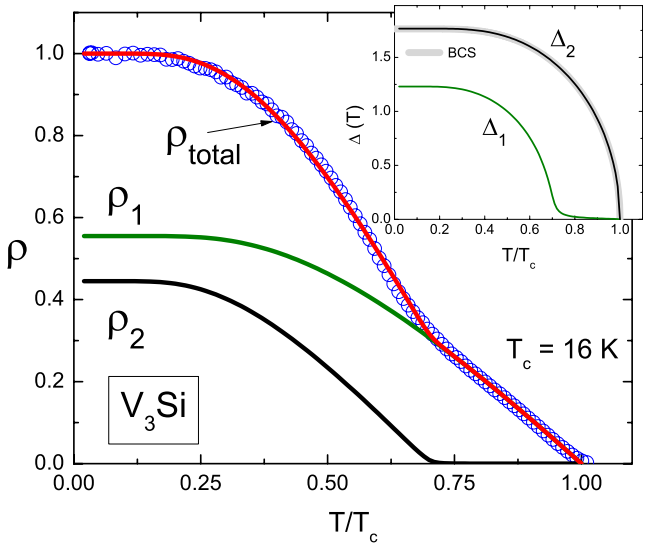

FIG. 4. (Color online) The data and fits of the superfluid density for V_3Si single crystal and corresponding temperature-dependent gaps (inset). The fitting parameters are $\lambda_{11}=0.1$, $\lambda_{22}=0.1$, $\lambda_{12}=1\times10^{-5}$, $n_1=0.47$, and $\gamma=0.4$.

$$\frac{F_n-F_s}{N(0)}=\frac{7\zeta(3)}{16\pi^2T_c^2}\sum_\nu n_\nu\Delta_\nu^4,$$

$$=7\zeta(3)\pi^2T_c^2\sum_\nu n_\nu\delta_\nu^4. \tag{24}$$

Following Ref. 14, one can look for solutions $\delta_\nu(t)$ of Eq. (20) near T_c as an expansion,

$$\delta_\nu=a_\nu\tau^{1/2}+b_\nu\tau^{3/2},\quad \tau=1-t. \tag{25}$$

We substitute this in Eq. (20) and compare terms of different powers of τ; the quantity $A_\mu=7\zeta(3)a_\mu^2\tau/2+\mathcal{O}(\tau^2)$. In the lowest order we obtain the system of linear homogeneous equations for $a_{1,2}$ that coincides with the system (11). The same arguments that led to Eq. (16) provide

$$a_2=a_1G=a_1\frac{\tilde{\lambda}-n_1\lambda_{11}}{n_2\lambda_{12}}. \tag{26}$$

The conditions for the existence of nontrivial solutions for b_ν in the next order provide the second relation for a_ν. We omit a cumbersome algebra and give the result

$$a_1^2=\frac{2}{7\zeta(3)}\frac{\tilde{\lambda}^2-n_1n_2\eta}{\tilde{\lambda}(n_1\lambda_{11}+n_2\lambda_{12}G^3)-n_1n_2\eta}. \tag{27}$$

We now obtain the energy near T_c,

$$F_n-F_s=7\zeta(3)N(0)\pi^2T_c^2\sum_\nu n_\nu a_\nu^4\tau^2=B\tau^2, \tag{28}$$

and the specific heat,

$$C_s-C_n=\frac{2B}{T_c}=14\zeta(3)\pi^2N(0)T_c\sum_\nu n_\nu a_\nu^4. \tag{29}$$

The relative jump at T_c is,

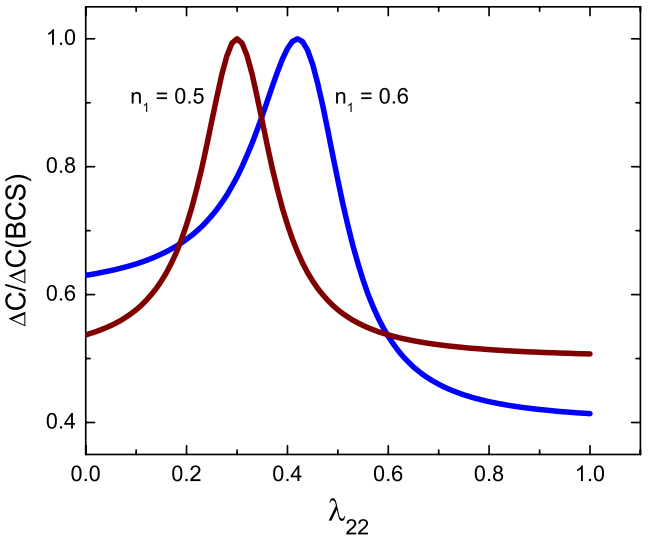

FIG. 5. (Color online) Dependence of the specific-heat jump on the mismatch between λ_{11} and λ_{22}. $\Delta C/C_N$ at T_c normalized on the BCS value of 1.43 is calculated using Eq. (30) with $\lambda_{11}=0.3$, $\lambda_{12}=0.06$, and two values of n_1 and plotted vs λ_{22}.

$$\frac{\Delta C}{C_n}=\frac{12}{7\zeta(3)}(n_1+n_2G^4)\left[\frac{\tilde{\lambda}^2-n_1n_2\eta}{\tilde{\lambda}(n_1\lambda_{11}+n_2\lambda_{12}G^3)-n_1n_2\eta}\right]^2. \tag{30}$$

If all coupling constants are the same, $\eta=0$, $G=1$, and $\Delta C/C_n=12/7\zeta(3)=1.43$, as is should be. We note that the sign of the interband coupling λ_{12} has no effect on the jump ΔC since in Eq. (30) $\lambda_{12}G$ is insensitive to this sign.

It is easy to study numerically the jump dependence on the three coupling parameters. As an example, we show in Fig. 5 the jump dependence on the mismatch between λ_{11} and λ_{22} for a fixed λ_{12} for two values of n_1. One can see that for equal relative densities of states, the jump peaks at $\lambda_{22}=\lambda_{11}$ at the one-band BCS value of 1.43; with the fixed λ_{11} and changing λ_{22} the jump drops with the mismatch $|\lambda_{22}-\lambda_{11}|$. The peak position and the drop speed vary with varying bands contributions so that the value of the jump per se cannot be interpreted as evidence for a particular order parameter.

Now we can test our model by employing parameters from the fit to the data on superfluid density (Fig. 3) to calculate the free energy and the specific heat. The result is shown in Fig. 6. The single-gap weak-coupling BCS specific heat is shown for comparison. The solid line is not a fit but a calculation with parameters determined in independent measurement. The data are taken from Ref. 16. Since this is *not* a fit, the agreement with the general behavior of $C(T)$ and, in particular, with value of the jump at T_c is remarkable.

IV. T_c SUPPRESSION BY NONMAGNETIC IMPURITIES

The intraband scattering does not affect T_c, so that we focus on the effect of interband scattering with an average scattering time τ. Since $g=1$ at T_c, the Eilenberger equations for $f_{1,2}$ in two bands read as[26]

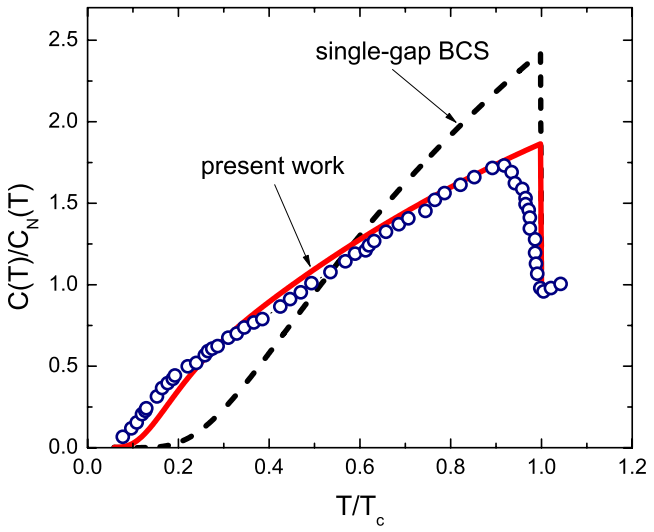

FIG. 6. (Color online) Normalized electronic specific heat $C(T)/C_N(T)$. Symbols are the data from Ref. 16. The solid line shows the result of the γ model; it is calculated using the energy (23) with parameters determined from the fit to the data on the superfluid density.

$$0 = 2\Delta_1 - 2\omega f_1 + \nu_2(f_2 - f_1)/\tau, \tag{31}$$

$$0 = 2\Delta_1 - 2\omega f_1 + \nu_2(f_2 - f_1)/\tau, \tag{32}$$

($\hbar = 1$). This system yields,

$$f_1 = \frac{\Delta_1(\omega + n_1/2\tau) + \Delta_2 n_2/2\tau)}{\omega\omega'}, \tag{33}$$

$$f_2 = \frac{\Delta_2(\omega + n_2/2\tau) + \Delta_1 n_1/2\tau)}{\omega\omega'}, \tag{34}$$

where $\omega' = \omega + 1/2\tau$. The self-consistency equation,

$$\Delta_\nu = \sum_{\mu,\omega} n_\mu \lambda_{\nu\mu} f_\mu, \tag{35}$$

again reduces to a system of linear and homogeneous equations for $\Delta_{1,2}$, the determinant of which must be zero. Omitting the algebra, we give the result,

$$P^2 n_1 n_2 \eta - P(n_1\lambda_{11} + n_2\lambda_{22} - n_1 n_2 \eta Q) + 1 - Q(n_1\eta_1 + n_2\eta_2) = 0, \tag{36}$$

$$\eta_1 = n_1\lambda_{11} + n_2\lambda_{12}, \quad \eta_2 = n_2\lambda_{22} + n_1\lambda_{12}, \tag{37}$$

η is defined in Eq. (12). The quantities P, Q are given by

$$P = \sum_\omega \frac{2\pi T_c}{\omega'} = \ln\frac{\omega_D}{2\pi T_c} - \psi\left(\frac{1}{2} + \frac{\rho_0}{2t}\right), \tag{38}$$

$$Q = \frac{1}{2\tau}\sum_\omega \frac{2\pi T}{\omega\omega'} = \psi\left(\frac{1}{2} + \frac{\rho_0}{2t}\right) - \psi\left(\frac{1}{2}\right), \tag{39}$$

where $t = T_c/T_{c0}$ with T_{c0} being the critical temperature of the clean material given in Eq. (14). The scattering parameter

$$\rho_0 = \frac{1}{2\pi T_{c0}\tau}. \tag{40}$$

One can easily rearrange P to the form,

$$P = \frac{1}{\tilde{\lambda}} - \ln t - Q. \tag{41}$$

Next, one solves the quadratic equation (36) for P and chooses the smaller of two roots (with the minus sign in front of the square root). Denoting this root as $P_r(\hat{\lambda}, \rho_0, t)$, where $\hat{\lambda}$ stands for the set of all coupling constants and of partial densities of states, we obtain an implicit equation for $t(\rho)$ that can be solved numerically,

$$\frac{1}{\tilde{\lambda}} - \ln t - Q(t,\rho) = P_r(\hat{\lambda}, \rho, t). \tag{42}$$

For the case $\eta = 0$, the only root of Eq. (36) is

$$P_r = \frac{1 - Q(n_1\eta_1 + n_2\eta_2)}{n_1\lambda_{11} + n_2\lambda_{22}}. \tag{43}$$

Since in this particular case $\tilde{\lambda} = n_1\lambda_{11} + n_2\lambda_{22}$, we obtain

$$-\ln t = Q\left(1 - \frac{n_1^2\lambda_{11} + 2n_1 n_2\lambda_{12} + n_2^2\lambda_{22}}{n_1\lambda_{11} + n_2\lambda_{22}}\right). \tag{44}$$

One can verify that this coincides with the suppression formula obtained within the model with factorizable coupling potential (see Ref. 22 or a more general work by Openov[27]). With the parentheses on the right-hand side equal to 1, this is just the Abrikosov-Gor'kov result for the T_c suppression by a pair breaker with the scattering parameter ρ_0. Thus, only if $n_1^2\lambda_{11} + 2n_1 n_2\lambda_{12} + n_2^2\lambda_{22} \le 0$, or

$$\lambda_{12} \le -\frac{n_1^2\lambda_{11} + n_2^2\lambda_{22}}{2n_1 n_2}, \tag{45}$$

T_c drops to zero at a finite τ. Otherwise, $T_c(\rho_0)$ is a decreasing function of ρ_0 that goes to zero as $\rho_0 \to \infty$.

One can show numerically that these features of the T_c suppression are qualitatively the same for a general two-band case: unlike formulas of preceding sections for clean materials, the sign of the interband coupling λ_{12} does affect the T_c suppression. One can verify that the interband scattering causes faster decrease in T_c if the interband coupling is repulsive, $\lambda_{12} < 0$.

To illustrate this point, we calculate suppression of T_c with the coupling parameters $\lambda_{11} = 0.3$, $\lambda_{22} = 0.2$, and with three different values of λ_{12} shown in Fig. 7. Whereas with positive λ_{12} the suppression is weak and similar to the case of materials having one anisotropic gap, the suppression for $\lambda_{12} < 0$ is much stronger.

This finding can be checked experimentally and, in fact, the recent data on unusually strong suppression of T_c with carbon, aluminum, or lithium doping[28] imply that MgB_2 might have repulsive interband coupling. Otherwise, it is hard to reconcile the T_c suppression by a factor of 4 by 15% of C substitution. If one interprets this effect as caused by impurities scattering, Eq. (42) with $\lambda_{12} = +0.06$ provides

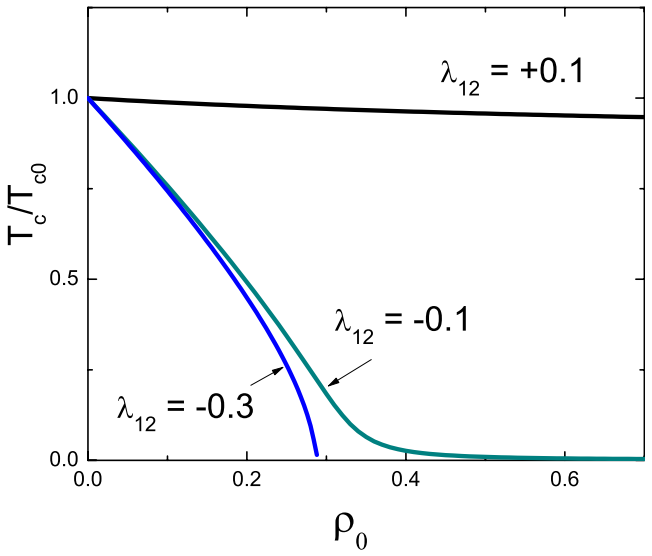

FIG. 7. (Color online) Suppression of the critical temperature by nonmagnetic impurities in a two-band superconductor. The intraband couplings $\lambda_{11}=0.3$ and $\lambda_{22}=0.2$ are the same for all curves. The suppression is much stronger when the sign of λ_{12} changes to negative (repulsive). For a strong repulsive λ_{12}, T_c turns zero at a finite scattering parameter ρ_0.

$\rho_0 \sim 10^3$ needed for such a suppression. This value of the scattering parameter corresponds to unrealistically short mean-free path $\ell \sim 1$ Å or less. Changing the sign of λ_{12} to negative (i.e., taking the interband coupling as repulsive), results in $\rho_0 \approx 0.37$ and a reasonable estimate of $\ell \approx 400$ Å. The negative interband coupling would imply opposite signs of the order parameter on the two effective bands of MgB_2, i.e., $\pm s$ order parameter, a verifiable proposition, given the recent experiments confirming $\pm s$ order parameter in iron pnictides.[29]

V. SUMMARY

We have presented a two-band weak-coupling γ model that takes into account self-consistently all relevant coupling constants to evaluate temperature dependencies of the two gaps, of the superfluid density, and of the specific heat in clean *s*-wave materials. The interband coupling is shown to have a strong effect on these dependencies irrespective of the sign of this coupling. In particular, if the interband coupling is negative (repulsive) it may cause the two order parameters to have opposite signs, i.e., the order parameter may have the $\pm s$ structure. In this case, the T_c suppression by interband scattering should be very strong; the feature that can be utilized as a signature of the $\pm s$ order parameter. We speculate that a strong T_c suppression by various dopants in MgB_2 may signal such a possibility. All these features make the model advantageous to the empiric and not self-consistent α model commonly employed to interpret the data on penetration depth and specific heat of two-gap materials.

ACKNOWLEDGMENTS

We thank R. T. Gordon and H. Kim for help with the experiments, J. Karpinski for MgB_2, and D. K. Christen for V_3Si single crystals, P. C. Canfield, A. Carrington, A. V. Chubukov, S. L. Bud'ko, A. J. Legett, I. I. Mazin, J. Schmalian, M. A. Tanatar, and Z. Tesanovic for interest and discussions. Work at the Ames Laboratory is supported by the Department of Energy-Basic Energy Sciences under Contract No. DE-AC02-07CH11358. R.P. acknowledges support of Alfred P. Sloan Foundation.

*kogan@ameslab.gov
†cmartin@ameslab.gov
‡Corresponding author; prozorov@ameslab.gov

[1] F. Bouquet, Y. Wang, R. A. Fisher, D. G. Hinks, J. D. Jorgensen, A. Junod, and N. E. Phillips, Europhys. Lett. **56**, 856 (2001).
[2] J. D. Fletcher, A. Carrington, O. J. Taylor, S. M. Kazakov, and J. Karpinski, Phys. Rev. Lett. **95**, 097005 (2005).
[3] J. D. Fletcher, A. Carrington, P. Diener, P. Rodiere, J. P. Brison, R. Prozorov, T. Olheiser, and R. W. Giannetta, Phys. Rev. Lett. **98**, 057003 (2007).
[4] Yu. A. Nefyodov, A. M. Shuvaev, and M. R. Trunin, Europhys. Lett. **72**, 638 (2005).
[5] V. A. Gasparov, N. S. Sidorov, and I. I. Zver'kova, Phys. Rev. B **73**, 094510 (2006).
[6] R. Prozorov and R. W. Giannetta, Supercond. Sci. Technol. **19**, R41 (2006).
[7] A. A. Golubov and I. I. Mazin, Phys. Rev. B **55**, 15146 (1997).
[8] A. A. Golubov, J. Kortus, O. V. Dolgov, O. Jepsen, Y. Kong, O. K. Andersen, B. J. Gibson, K. Ahn, and R. K. Kremer, J. Phys.: Condens. Matter **14**, 1353 (2002).
[9] A. Brinkman, A. A. Golubov, H. Rogalla, O. V. Dolgov, J. Kortus, Y. Kong, O. Jepsen, and O. K. Andersen, Phys. Rev. B **65**, 180517(R) (2002).
[10] A. A. Golubov, A. Brinkman, O. V. Dolgov, J. Kortus, and O. Jepsen, Phys. Rev. B **66**, 054524 (2002).
[11] B. Mitrović, J. Phys.: Condens. Matter **16**, 9013 (2004).
[12] O. V. Dolgov, R. K. Kremer, J. Kortus, A. A. Golubov, and S. V. Shulga, Phys. Rev. B **72**, 024504 (2005).
[13] E. J. Nicol and J. P. Carbotte, Phys. Rev. B **71**, 054501 (2005).
[14] V. A. Moskalenko, Phys. Met. Metallogr. **8**, 503 (1959).
[15] H. Suhl, B. T. Matthias, and L. R. Walker, Phys. Rev. Lett. **3**, 552 (1959).
[16] Y. Wang, T. Plackowski, and A. Junod, Physica C **355**, 179 (2001).
[17] R. Prozorov, R. W. Giannetta, A. Carrington, and F. M. Araujo-Moreira, Phys. Rev. B **62**, 115 (2000).
[18] G. Eilenberger, Z. Phys. A **214**, 195 (1968).
[19] B. T. Geilikman, Usp. Fiz. Nauk **88**, 327 (1966) [Sov. Phys. Usp. **9**, 142 (1966)].
[20] I. I. Mazin and J. Schmalian, Physica C **469**, 614 (2009).
[21] D. Markowitz and L. P. Kadanoff, Phys. Rev. **131**, 563 (1963).
[22] V. G. Kogan, Phys. Rev. B **66**, 020509(R) (2002).

[23] H. J. Choi, D. Roundy, H. Sun, M. L. Cohen, and S. G. Louie, Phys. Rev. B **66**, 020513(R) (2002).
[24] K. D. Belashchenko, M. van Schilfgaarde, and V. P. Antropov, Phys. Rev. B **64**, 092503 (2001).
[25] J. C. Lagarias, J. A. Reeds, M. H. Wright, and P. E. Wright, SIAM J. Optim. **9**, 112 (1998).
[26] V. G. Kogan and N. V. Zhelezina, Phys. Rev. B **69**, 132506 (2004).
[27] L. A. Openov, Pis'ma Zh. Eksp. Teor. Fiz. **66**, 627 (1997) [JETP Lett. **66**, 661 (1997)].
[28] S. M. Kazakov, R. Puzniak, K. Rogacki, A. V. Mironov, N. D. Zhigadlo, J. Jun, Ch. Soltmann, B. Batlogg, and J. Karpinski, Phys. Rev. B **71**, 024533 (2005).
[29] C. T. Chen, C. C. Tsuei, M. B. Ketchen, Z. A. Ren, and Z. X. Zhao, arXiv:0905.3571 (unpublished).